Transient non-thermal mobility of monomer in a superficial monomer–trimer catalytic reaction: a Monte Carlo simulation study

2002 J. Phys.: Condens. Matter 14 7177

(http://iopscience.iop.org/0953-8984/14/30/308)

INSTITUTE OF PHYSICS PUBLISHING JOURNAL OF PHYSICS: CONDENSED MATTER

J. Phys.: Condens. Matter **14** (2002) 7177–7190 PII: S0953-8984(02)33506-9

Transient non-thermal mobility of monomer in a superficial monomer–trimer catalytic reaction: a Monte Carlo simulation study

K M Khan, P Ahmad and K Iqbal

Nuclear Physics Division, Pakistan Institute of Nuclear Science and Technology, PO Nilore, Islamabad, Pakistan

Received 6 February 2002, in final form 13 May 2002
Published 17 July 2002
Online at stacks.iop.org/JPhysCM/14/7177

Abstract

The phase diagram of the monomer–trimer model has already been studied on the basis of (a thermal) Langmuir–Hinshelwood (LH) mechanism, the details of which can be found in the literature. Here, we have studied the transient non-thermal mobility of monomer based on Eley–Rideal (ER) and precursor mechanisms. With the introduction of the ER process, the continuous transition of the LH model has been eliminated and production rate has been increased. The production rate can be represented by simple mathematical equations. Introduction of the precursor process reveals a phase diagram similar to the monomer–dimer precursor model. The reactive window width increases with an increase in the precursor mobility. When the precursor mobility is increased to the third-nearest neighbourhood a situation similar to the ER model is reproduced. The effect of monomer diffusion and desorption has also been studied for ER and precursor models. Results have been compared and some interesting observations have been reported.

1. Introduction

The knowledge of the details of catalytic reaction systems is generally of great chemical and industrial significance. The scientific interest in the study of these processes is due to the emergence of a rich and complex variety of physical chemistry phenomena including, e.g., critical phenomena and irreversible phase transitions (IPTs), propagation and interference of chemical waves of adsorbed reactants etc. The detailed understanding of such catalytic reactions is very important in applied research but such an understanding has rarely been achieved either from the experiment or from theory. An investigation of the lattice models of the catalytic surface reactions has been extremely helpful in gaining a better understanding of the kinetics of catalytic processes. Ziff *et al* [1] and Dumont *et al* [2] introduced a monomer–dimer (MD) model, which has been used to study a reaction system of the type $2A+B_2 \rightarrow 2AB$. This reaction mimics the catalytic oxidation of CO. This model is generally known as the

0953-8984/02/307177+14$30.00

ZGB model. In this model a square lattice models the surface, and as a function of the feed concentration y_A of the monomer (A) the system exhibits continuous (y_1) and discontinuous (y_2) phase transitions at $y_A = 0.389 \pm 0.001$ and $y_A = 0.525 \pm 0.001$, respectively. Within the window defined by $y_1 < y_A < y_2$ the system exhibits a steady reactive state (SRS) with the continuous production of AB. Ever since this seminal work a number of authors have modified this model to study different reaction systems of interest [3–17]. Meakin and Scalapino [3] investigated the effect of the lattice type on the reactive window of the ZGB model. They found that for a hexagonal lattice (each surface site has six nearest neighbours) the reactive window increases in size as compared with the usual square lattice with $y_1 = 0.360 \pm 0.005$ and $y_2 = 0.561 \pm 0.001$.

The kinetics of irreversible dimer–dimer surface reaction of the type $A_2 + B_2 \rightarrow 2AB$ with desorption of dimer B_2 has been studied by Khan *et al* [4] on a square lattice. For the desorption probability (P) of B_2 equal to zero, a single discontinuous transition separating an A+ vacancies saturated surface from a B+ vacancies saturated surface is obtained at $y_B = 0.50$ (y_B is the feed concentration of dimer B_2). With the increase in P an SRS, separated from the poisoned state by two continuous transitions, is obtained for this system. The position of the transition points depends upon the value of P. Kohler and ben-Avraham [5] have reported the results of a hypothetical dimer–trimer (DT) model of the type $3A_2 + 2B_3 \rightarrow 6AB$ on a hexagonal lattice. They have observed a phase diagram in which an SRS is separated from a B+ vacancies poisoned state by a continuous transition (y_1) and an A+ vacancies poisoned state by a discontinuous transition (y_2). The phase diagram seems to resemble the standard ZGB model qualitatively, with the difference that for $y_A < y_1$ ($> y_2$) in the ZGB model the surface is poisoned with 100% B (A). However, a number of discrepancies can be found in their paper [6]. Khan *et al* [6] have studied the same model on a square surface. The lattice type has a significant effect on the reactive window of the system. The reactive window width of ≈ 0.12 (as shown by Kohler and ben-Avraham for the hexagonal case) has been significantly reduced to ≈ 0.02 for the square lattice. Khan *et al* [6, 7] have also studied a hypothetical monomer–trimer (MT) model of the type $3A + B_3 \rightarrow 3AB$ on the square and hexagonal surfaces. Their model is based on the Langmuir–Hinshelwood (LH) mechanism. The model reveals a phase diagram which is very similar to that of the ZGB model. For the square lattice, the values of continuous (y_1) and discontinuous (y_2) phase transition points are 0.190 ± 0.005 and 0.465 ± 0.005, respectively. On moving from the square to the hexagonal lattice, the general features of the phase diagram remain the same. The value of y_1 remains almost the same, whereas the value of y_2 shifts from 0.465 to 0.525 ± 0.005.

The transient non-thermal mobility caused by the inability to dissipate the energy instantaneously gained by a particle after the formation of a surface bond seems to be a common process in nature. One class of such catalysed reactions is envisaged to proceed through the Eley–Rideal (ER) mechanism, in which a gas phase reactant, never in equilibrium with the surface, directly picks up a fragment of the adsorbed reactant and forms a product, which leaves the surface. This class of reaction, halfway between the gas phase type and the LH type, is of interest in surface science. Jackson and Persson [18] have studied the dynamics of a 'hot' hydrogen dimer in the ER process (a direct reaction between a gas phase H atom and an adsorbed H atom) using a fully three-dimensional flat surface model for Cu(111). Meakin [19] has explored the effects of the ER process on the simple ZGB model for the catalytic oxidation of CO by oxygen. The ER process results in the formation of a new regime in which a continuous reaction can be sustained. The moment CO partial pressure departs from zero a continuous production of CO_2 starts. This production continues until $y_{CO} \approx 0.497$, where a first-order phase transition terminates this activity and the surface is poisoned by CO. Utilizing the ER process, he has also studied the monomer–monomer reaction system and obtained

similar results. Very recently, Khan and Ahmad [31] have explored the effects of the ER mechanism on a simple LH model for the NO–CO catalytic reaction on a square surface. The usual chequerboarding process of N atoms on the surface of a square lattice has been broken down. The moment CO partial pressure (y_{CO}) departs from zero, continuous production of CO_2 and N_2 starts until $y_{CO} = 0.034$; a very small reactive window. For $y_{CO} > 0.034$, the catalytic activity stops and the surface is poisoned with a combination of CO and N. Diffusion of CO on the surface further reduces the width of the reactive region. However, diffusion of N atoms widens the reactive window width significantly. With the introduction of a small CO desorption probability ($\approx$0.01), the situation changes completely. The system reveals a phase diagram with two transition points ($y_1 \approx 0.20$ and $y_2 \approx 0.32$), which is qualitatively similar to the ZGB model (where $y_1 \approx 0.395$ and $y_2 \approx 0.525$). The width of the reactive window initially increases with increase in CO desorption probability and then attains an almost constant value.

The other class of heterogeneous catalysed reactions is the precursor mechanism. Harris and Kasemo [20] have given arguments in favour of a precursor mechanism for surface reactions involving direct collisions between chemisorbed species and molecules or atoms that are trapped in the neighbourhood of the surface but have not thermalized. The precursor mechanism is generally different from LH or ER mechanisms [20–22]. Based on the precursor mechanism Khan *et al* [23] have recently studied the catalytic production of water along the lines visualized by Harris and Kasemo [20] through Monte Carlo (MC) simulations. This work introduces some interesting features in the phase diagram of the catalytic dimer–dimer reaction, which were not seen by considering the LH mechanism only [10]. The model shows a steady reactive region, which is limited by the continuous and discontinuous IPTs. The phase diagram is similar to that of the ZGB model qualitatively; however, the width of the reactive region increases if the motion of the precursor is extended to the second and third neighbourhood. Some experimentally known facts, such as the occurrence of first-order transitions and the dependence of the reaction rate on the oxygen coverage, are also observed in this model. Khan *et al* [17, 24] have also studied the catalytic formation of ammonia based on a hot hydrogen precursor as suggested by Harris and Kasemo [20]. The most striking feature of this study is the occurrence of a steady reactive region with continuous production of NH_3, which was not observed in the LH (ZGB-like) model. The results of the model of Khan *et al* [17, 24] are qualitatively similar to those observed in the ZGB model, i.e. the reactive window width and the nature of the IPTs are the same. Very recently, the study of an MD system [30] based on a non-thermal model involving the precursor motion of the monomer (CO) has divulged that the continuous transition disappears when the mobility of the precursor is extended to the third-nearest neighbourhood.

The objective of this paper is to investigate the effects of the ER and precursor mechanisms on the phase diagram of a hypothetical (superficial) MT surface catalytic reaction system. We shall also study the effect of diffusion and desorption of the monomer on the phase diagram of the system. The sole purpose of this study is to obtain a theoretical knowledge of the behaviour of the species on the surface so that more real but complicated MT systems such as those for the water gas shift reaction may be studied with better understanding. The paper is structured as follows: in the next section, the reaction model and the simulation procedure will be discussed. The results will be presented and discussed in section 3. Finally, the conclusions will be drawn in section 4.

2. Model and simulation

Let us divide this section into two parts. In the first part, we shall give the simulation details of the ER model, whereas in the second part the precursor model will be discussed.

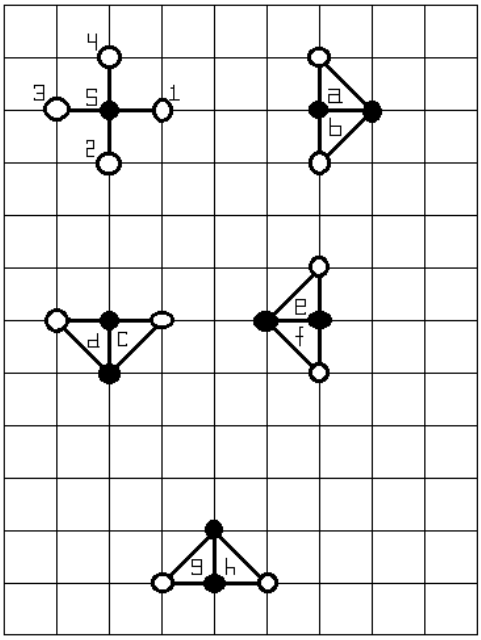

Figure 1. Four nearest neighbours of surface site S are marked as 1, 2, 3 and 4. Different possible choices of a trimer adsorption on a square lattice forming vertices of a right-angled triangle are shown by a, b, c, d, e, f, g and h. See the text for details.

The relative partial pressures of A and B_3 are y_A and $1 - y_A$ respectively. We consider the square lattice of size $L = 128$. It is observed that an increase in the lattice size changes the critical values slightly but the overall qualitative nature of the phase diagram is not affected [4, 10]. The simulation starts with a clean surface. To make the lattice infinite we use the periodic boundary conditions. The four nearest-neighbouring (nn) sites of the selected site S are shown in figure 1. The equilibrium coverages are measured as a function of the partial pressure of A (y_A). In order to locate the critical points ten independent runs, each up to 50 000 MC cycles, are carried out. If the ten runs proceed up to 50 000 MC cycles without the lattice being poisoned, the particular point is considered to be in the SRS. The poisoning of even a single run is a sufficient criterion for considering the point in the poisoned state. If the run does not end up in a poisoned state, then in order to obtain the coverages in the SRS the initial 10 000 MC cycles are ignored and the system is allowed to run up to 50 000 MC cycles. The values of the coverage and the production rate are obtained after every ten MC cycles, so that the final coverage (production rate) is an average of 4000 points.

2.1. Eley–Rideal model

We propose the LH MT model of the type $3A + B_3 \rightarrow 3AB$. It is symbolically represented by the following four equations [6]:

$$A(g) + S \rightarrow A^s \tag{1}$$

$$B_3(g) + 3S \rightarrow 3B^s \tag{2}$$

$$A^s + B^s \rightarrow AB(g) + 2S. \tag{3}$$

With the introduction of the ER process, one has to add the following equation:

$$A(g) + B^S \rightarrow AB(g) + S \tag{4}$$

where S is an empty surface site, (g) refers to the gas phase and X^S represents the X adatom. There appears to be a considerable uncertainty concerning the relative importance of the LH and ER reaction steps given by equations (3) and (4) respectively [25, 26]. It is worthwhile to mention that the relative frequency of the LH reaction step and the ER reaction step depends upon the trimer coverage. If the initial trimer coverage on the surface is higher (small y_A values) then the ER reaction step becomes dominant; otherwise the LH reaction step becomes important [26]. Consequently, it seems worthwhile to investigate the addition of reaction step (4) to the usual simple LH model of the reaction system.

The simulation proceeds as follows: the monomer (A) adsorption trial is performed with probability y_A whereas that of B_3 is performed with probability $1 - y_A$.

(a) If a trimer happens to be adsorbed, a surface site is chosen randomly. If the site is occupied then the trial ends, else two more vacant sites are scanned. The choice of the two sites (after the initial selection of an empty site S) is made in such a way that the three sites constitute the vertices of a right-angled triangle (figure 1). If these randomly chosen sites are empty, then B_3 is adsorbed in atomic form on these sites. The adsorption of a trimer on triplets of linear vacancies is not allowed. There are two sets of triplets of linear vacancies, as shown by (1, S, 3) and (2, S, 4) in figure 1. After adsorption, all four nn sites are scanned randomly for an A adatom. If any of the four sites has an A, then the B adatom reacts with A forming AB, and the two sites are evacuated.

(b) If the monomer A happens to be selected, there are two possibilities. Either the site is occupied or it is empty. If the selected site is occupied by a species other than a B atom, the trial ends. If B occupies it, reaction step (4) takes place with some probability E_A, where E_A is the probability of the ER reaction.

(c) If the randomly selected site is vacant, then the monomer A adsorbs on it. After adsorption, all four nn sites are scanned randomly for B. If any of the four sites has a B, then the A adatom reacts with B forming AB, and the two sites are vacated. The variables in our (diffusionless) simulation are y_A and E_A.

In order to introduce the diffusion of the A species, we have modified the simulation slightly. If reaction step (3) does not take place after the monomer A adsorption then one of its four nn sites is picked randomly. If this randomly selected site is occupied then the trial ends. If the randomly selected site is vacant, the monomer A diffuses to this vacant site with some probability d_A. After diffusion the possibility of reaction step (3) is again checked. All the rest of the simulation procedure is the same as discussed earlier. Therefore, in this study y_A and d_A are the two variables. We have studied the diffusion of species A for a fixed particular value of E_A.

In a similar way, a slight modification in the (diffusionless) simulation procedure is made in order to incorporate desorption of the monomer. If at the beginning the selected site is occupied by an A adatom then the possibility of its desorption is examined with the desorption probability P_A. In order to do this, a random number is generated and is compared with P_A. If it is less than P_A then the A adatom leaves the surface and the site is vacated, otherwise the trial ends. The rest of the simulation procedure is the same as discussed earlier. In this study, y_A and P_A are the two variables.

2.2. Precursor mechanism

We may write the equations for this reaction system, which incorporates the precursor mechanism, as follows.

$$B_3(g) + 3S \rightarrow 3B^C \tag{5}$$

$$A(g) + S \rightarrow A^P + S \tag{6}$$

$$A^P + B^C \rightarrow AB(g) + S \tag{7}$$

$$A^P + S \rightarrow A^C \tag{8}$$

$$A^C + B^C \rightarrow AB(g) + 2S \tag{9}$$

where (g) indicates the species in the gas phase and S is a vacant surface site. X^P and X^C represent the precursor and chemisorbed species, respectively.

The simulation starts with a clean surface. If the striking molecule is A, then it requires only one vacant site in order to produce a precursor A^P (equation (6)). If the striking molecule is B_3, then it requires three vacant sites in order to produce three chemisorbed atoms B^C (equation (5)). We shall study the motion of a precursor (and its collision with the chemisorbed species) up to the first-, second- and third-nearest neighbourhood. However, the reaction between two chemisorbed species will be restricted to the first-nearest neighbourhood. Therefore, in our simulation there are two parameters: y_A and R, which is the range of the neighbourhood visited by the precursor. The equilibrium coverages are measured as a function of y_A. The steps involved in the simulation are as follows: a site is picked randomly. If the site is occupied the trial ends (the molecule is backscattered), else the collision of molecules A and B_3 is considered with probability y_A and $1 - y_A$, respectively.

(a) If the colliding molecule is B_3 then its adsorption is performed in the same way as discussed in the above model of the system.

(b) If the colliding molecule is A then, after collision with this randomly chosen site, precursor A^P is produced via step (6), which moves into the 'environment' with a range R. We have considered three different ranges of this environment:

  (i) first-nearest neighbourhood ($R = d$)
  (ii) second-nearest neighbourhood ($R = \sqrt{2}d$) and
  (iii) third-nearest neighbourhood ($R = 2d$), where d is the lattice constant.

  Each environment consists of a specific pattern of the set of sites around the striking site. For example, the first environment consists of four nn sites. The second environment contains four nn and four second-nn sites whereas the third environment contains all eight sites of the second environment and an additional four third-nn sites.

(c) If during its motion in a particular environment a precursor A^P strikes a chemisorbed atom B^C then reaction step (7) takes place and the precursor ends its life. If the precursor does not find any chemisorbed reacting species within the range R then it takes one vacant site (randomly chosen) from the environment to be chemisorbed (step (8)) and the precursor ends its life. This chemisorbed atom scans its four nn sites for the presence of B^C in order to complete reaction step (9). If B^C is found then AB(g) is formed, which desorbs and two sites are vacated. It should be noted that after adsorption the B^C atoms also scan their first-nearest neighbourhood in order to complete the possible reaction step (9).

(d) If the precursor does not end its life through any of the above-mentioned ways, then it returns to gas phase and hence the trial ends.

In order to introduce the diffusion and desorption of the A species, we have modified the simulation procedure of the first environment in a similar way as discussed in model 1.

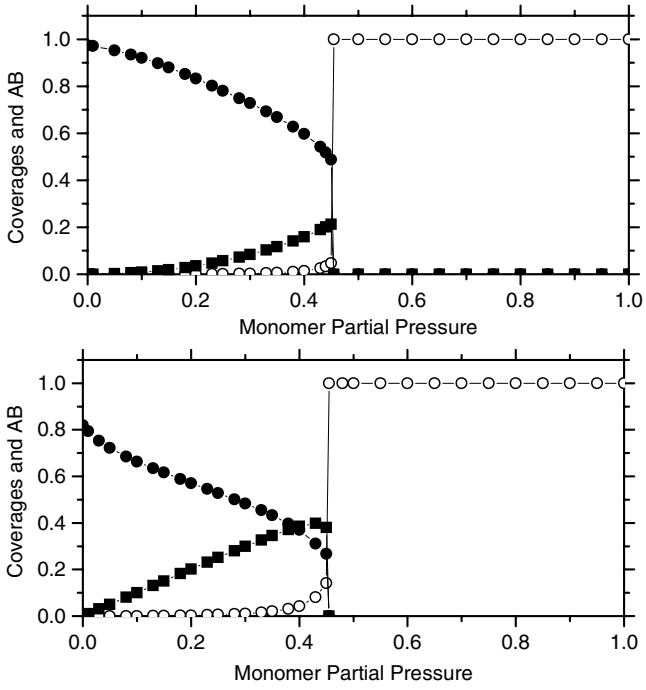

Figure 2. Coverages of trimer (solid circle) and monomer (open circle) and production of AB (solid square) plotted as functions of monomer partial pressure for model 1 for $E_A = 0.01$ (top) and $E_A = 1.0$ (bottom). The diffusion and desorption of monomer are ignored.

We have not considered the diffusion or desorption of the A species in the second and third environments of the model.

3. Results and discussion

If reaction step (4) in model 1 is ignored then the results are well known [6]. In this case IPTs at $y_1 = 0.185 \pm 005$ and $y_2 = 0.455 \pm 0.005$ are observed. Therefore, the system exhibits a reactive window of the order of ≈0.27. The nature of these IPTs is second order (continuous) and first order (discontinuous), respectively. For $y_A < y_1$ the surface is completely covered by B atoms, whereas for $y_A > y_2$ it is completely covered by A. However, the situation changes when reaction step (4) is considered with some probability E_A. It is interesting to note that a very slight value of E_A (≈0.01) eliminates the continuous transition (figure 2), whereas the value of y_2 remains the same. With further increase in E_A, the values of transition points (and hence the reactive window width) and the qualitative nature of the phase diagram are unchanged as is evident from figure 2, which shows the situations when reaction step (4) is considered with probability 0.01 (top) and 1.0 (bottom) respectively. However, the maximum production rate increases with increase in E_A. Figure 3 shows behaviour of the type $R_{max} = 0.213\,98 + 0.293\,19E_A - 0.112\,38E_A^2$. This is expected because by increasing E_A we are actually increasing the probability of reaction step (4), which results in more production.

Figure 2 shows that the continuous production of AB starts as soon as the monomer partial pressure and E_A departs from zero, and remains until $y_A = 0.4550 \pm 0.005$, where a discontinuous phase transition (y_2) stops the catalytic activity. This situation is completely

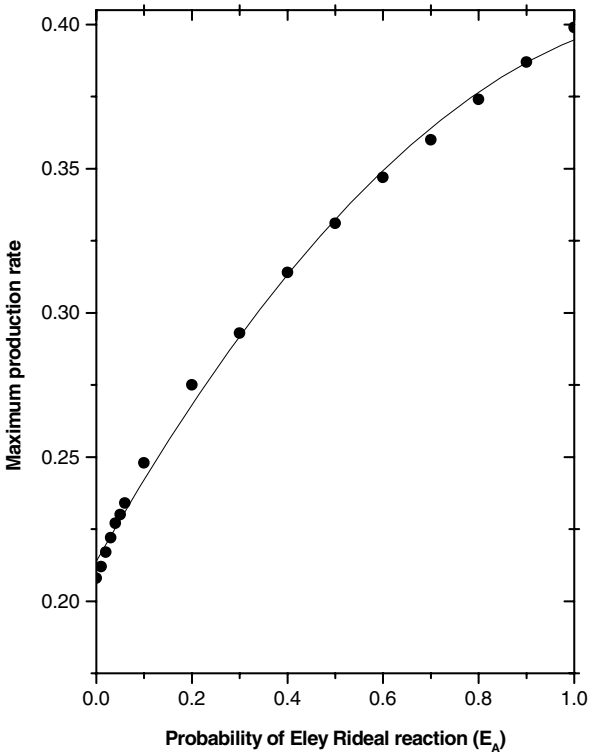

Figure 3. The maximum production rate is plotted as a function of probability of the ER reaction step (E_{A}) for model 1.

different from that observed in the LH MT model ($E_{\mathrm{A}} = d_{\mathrm{A}} = P_{\mathrm{A}} = 0$), which reveals a phase diagram similar to the ZGB model [6]. In our present model, for lower monomer (higher trimer) partial pressures, the surface contains clusters of B atoms. In this region, reaction step (4) on one hand burns the chemisorbed B atoms of these clusters whereas on the other hand it creates isolated vacancies inside these clusters. On these isolated vacancies the monomer can be chemisorbed easily, which can trigger reaction step (3) too. In this way, B atoms burn very quickly. The generation of isolated vacancies (due to ER reaction step (4)) precludes the adsorption of the trimers and therefore the continuous transition is eliminated, i.e. the production starts the moment y_{A} departs from zero. These results show that due to reaction step (4) the reactivity becomes very high in the region where the coverage of the adsorbed trimer is the highest and vice versa. This proves the fact that the ER reaction step becomes more dominant when the trimer coverage is high, otherwise the LH reaction step becomes important, which is compatible with the literature [26]. Our simulation results closely resemble the results of Meakin [19] and Khan *et al* [31] for MD ER models. Therefore, we conclude that the behaviour of our (MT) ER model is very similar to that of the MD ER model.

With introduction of diffusion in model 1 for a fixed E_{A} both the window width (W) and the production rate R_{max} increase with the diffusion probability (d_{A}) of the monomer. Figure 4 shows the situation for a fixed $E_{\mathrm{A}} = 0.5$ (top) and $E_{\mathrm{A}} = 1.0$ (bottom). For $E_{\mathrm{A}} = 0.5$, the equation of fit for window width is $W = 0.443\,29 + 0.044\,28\ (d_{\mathrm{A}}) + 0.008\,62\ (d_{\mathrm{A}}^2)$ and that for maximum production rate is $R_{max} = 0.398\,13 + 0.063\,21(d_{\mathrm{A}}) + 0.003\,61\ (d_{\mathrm{A}}^2)$. For $E_{\mathrm{A}} = 1.0$,

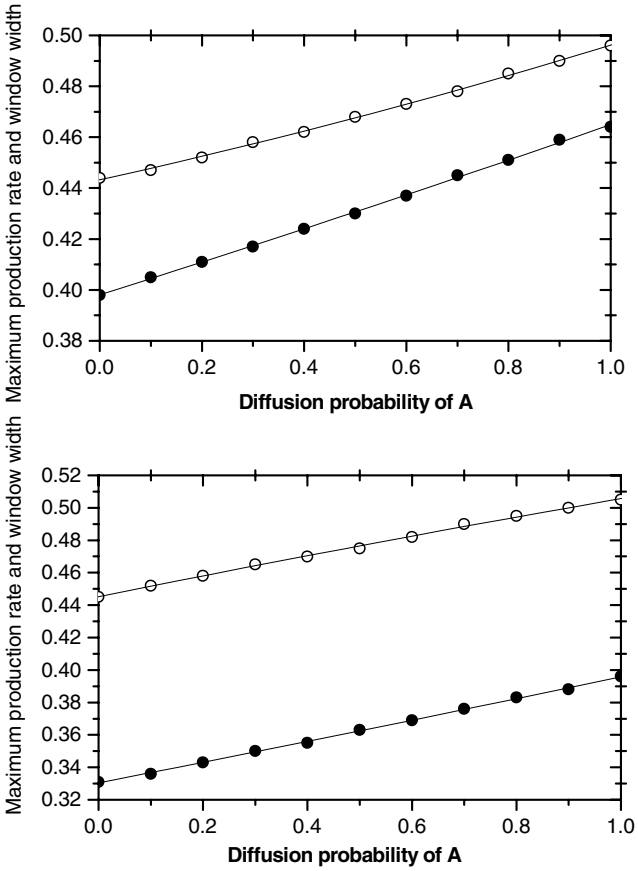

Figure 4. Maximum production rate (solid circle) and window width (open circle) plotted versus diffusion probability of A for model 1 for $E_A = 0.5$ (top) and $E_A = 1.0$ (bottom).

the equation of fit of window width is $W = 0.443\,95 + 0.069\,72\ (d_A) - 0.006\,99\ (d_A^2)$ and that of maximum production rate is $R_{max} = 0.330\,41 + 0.062\,92\ (d_A) + 0.002\,45\ (d_A^2)$. Since diffusion increases the reactivity of the monomer by giving yet another chance of reaction step (9), it increases both the window width and the maximum production rate.

Figure 5 (top) shows the case corresponding to the first environment of model 2 (diffusion and desorption of the monomer are ignored), where coverages of the species and production of AB are plotted as a function of y_A. In this case IPTs at $y_1 = 0.185 \pm 005$ and $y_2 = 0.515 \pm 0.005$ are observed, showing a reactive window of the order of ≈ 0.33. The nature of these IPTs is second order (continuous) and first order (discontinuous), respectively. For $y_A < y_1$ the surface is completely covered by B atoms, whereas for $y_A > y_2$ it is completely covered by A atoms. This shows that the introduction of equations (6) and (7) in the LH model does not have any significant qualitative effect on the phase diagram of the reaction system [6]. The value of transition point y_1 is same as that of the LH model. This is because, as in the LH model, in this region nearly every A impinging on the surface reacts with B atoms to form AB(g). However, the value of transition point y_2 is larger than that of the LH model [6]. This effect can be understood by the fact that, in the LH model, A must be chemisorbed on the site of impact (say S). This chemisorbed A can pick B^C from the first-nearest neighbourhood only. On the

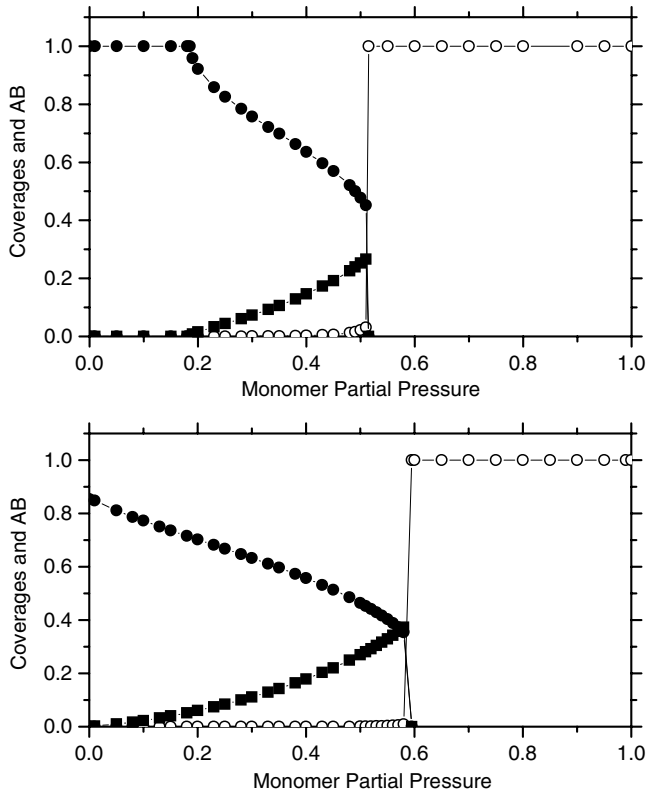

Figure 5. Coverages of trimer (solid circle) and monomer (open circle) and production of AB (solid square) plotted as functions of monomer partial pressure for model 2 for the first environment (top) and for the third environment (bottom). The diffusion and desorption of monomer are ignored.

other hand, in model 2 the precursor atom may be chemisorbed on a site different from the site of impact S. When the precursor A picks a site from the nearest neighbourhood of S in order to be chemisorbed, it will react with B^S sitting in the second-or third-nearest neighbourhood of S. Therefore, such a diffusive character of A increases its reactivity and y_2 is shifted towards a higher value of y_A.

When the precursor motion is considered up to the second environment, the values of y_1 and y_2 are 0.130 ± 0.005 and 0.560 ± 0.005 respectively, with a window width of the order of ≈ 0.43, which is significantly larger than that in the previous case. The lower half of figure 5 shows the situation when the third environment is considered. Here the second-order transition disappears. When y_A is zero, the surface is covered by B atoms (≈ 0.86) and isolated vacancies (≈ 0.14) (random trimer filling). The moment y_A becomes non-zero (say $y_A = 0.005$), the formation of AB takes place which continues to increase up to y_2, where it drops rapidly to zero and the surface is completely covered by A. It should be noted that in the third environment starting from $y_A = 0$, even for a small value of y_A such as $y_A = 0.005$, there is a sudden jump to the continuous reaction state. Thus, $y_A \approx 0$ is a first-order transition point from poisoned to SRS. The value of y_2 is 0.595 ± 0.005.

It has been observed that at lower monomer partial pressures (higher trimer partial pressures) the B atoms form ordered islands and eventually poison the surface. In the first environment of our model, for the region close to y_1, the monomers (precursors) start burning

B atoms at the perimeters of B islands. However, the hopping of A^P into the second environment burns more B atoms inside the B islands and creates more single vacant sites (due to B^S–A^P reaction) inside the B islands. Therefore, the supply of A gas is increased indirectly, which will require more B atoms to burn and hence y_1 shifts towards lower values of y_A. For the region close to y_2, in the higher environment, fewer A^P precursors are ending their life as A^S molecules (due to increased A^P reactivity) as compared with the first environment and hence B_3 molecules can find more vacancy pairs for adsorption. Therefore, y_2 shifts towards higher values of y_A.

The shift of the transition region towards higher monomer pressure with the consequent enhancement of monomer reactivity is in good agreement with the experimental situation of the LH MD model as observed by Ehsasi *et al* [27]. This experimental fact has also been confirmed by the computer simulation results [15, 27, 28]. Ehsasi *et al* [27] have shown that the monomer diffusion results in a higher reactivity of the monomer, which shifts the discontinuous transition point to a higher monomer partial pressure. They have shown that by considering large monomer diffusion y_2 shifts towards the stoichiometric value $2/3$. Khan *et al* [15, 28] have also shown that introduction of a subsurface in the ZGB model plays the same role as played by diffusion in the work of Ehsasi *et al* [27], namely it increases the reactivity of the monomer, which subsequently shifts the discontinuous transition point to higher monomer partial pressure. However, Evans has shown that in the infinite-diffusion-rate limit $2/3$ represents the spinodal rather than the true transition point [29]. He also claims that true transition point for the MD model is ≈ 0.595. Khan *et al* [30] have seen that the precursor model of a MD system yields the same value (≈ 0.595) when the precursor motion of the monomer is extended to the third environment. This value is the same as claimed by Evans [29] to be the true transition point for the MD model. Remarkably, the same value of y_2 (≈ 0.595) is obtained when the mobility of the monomer is extended to the third environment in our present precursor model. This shows that the present MT model behaves similarly to the MD precursor model of Khan *et al* [30].

When diffusion is considered both the production rate R_{max} and the window width W increase with the increase in diffusion probability d_A in model 2 as shown in figure 6 (top). Since diffusion enhances the reactivity of the monomer it therefore not only shifts y_2 towards the right (increased window width W) but also increases the production rate R_{max} when compared with figure 5 (top).

Figure 6 (bottom) shows mathematical fits of the data of production rate (R) versus monomer partial pressure (y_A) for model 1 and the first environment of model 2 when diffusion and desorption of monomer are ignored. The equations of the fits are $R = -0.005\,49 + 1.1253\,(y_A) - 0.390\,52(y_A)^2$ and $R = -0.002\,01 - 0.152\,79\,(y_A) + 1.316\,23(y_A)^2$ in model 1 and the first environment of model 2, respectively. The standard deviations of the data are 0.003 46 and 0.002 69, respectively. When diffusion of the monomer is introduced into the two models, mathematical fits of the data of production rate versus monomer partial pressure (y_A) show similar behaviour as shown in figure 6 (bottom). The equations of fits are $R = -0.002\,94 + 1.079\,39\,(y_A) - 0.211\,07\,(y_A)^2$ and $R = -0.009\,32\,0.110\,42\,(y_A) + 1.2416\,(y_A)^2$ in model 1 and the first environment of model 2, respectively. The standard deviations of the data are 0.0037 and 0.0034, respectively. A similar fit is also obtained for the data of the second environment, which can be given by $R = 0.0044 - 0.131\ y_A + 1.238\ (y_A)^2$ (with standard deviation ≈ 0.0047). However, the data of the third environment are well satisfied by an exponential relation of the type $R = 0.011 \exp(6.65 y_A)$ (with chi squared ≈ 0.0001). The change of behaviour from polynomial to exponential is due to the increased reactivity of monomer in the third environment. It is also interesting to note that the production of AB is significantly larger in model 1 than in the first environment of model 2.

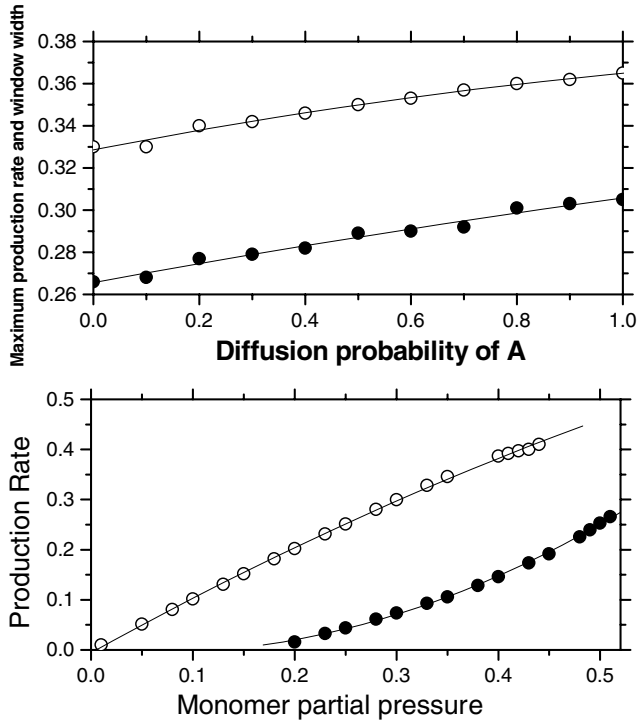

Figure 6. The upper half of the figure shows the maximum production rate (solid circle) and window width (open circle) plotted versus diffusion probability of A for the model 2 first environment (top). The lower half of the figure shows the production rate of the model 2 first environment (solid circle) and of model 1 (open circle) when diffusion and desorption are ignored.

With the introduction of desorption of the monomer with probability (P_A), the situation significantly changes in the two models, as shown in figure 7. In the ER model (top), with increase in P_A, the values of y_1 remain unchanged whereas the values of y_2 increase towards higher monomer partial pressure until $P_A = 0.20$ and thereafter y_2 takes a fixed value (=1). For $P_A > 0.20$ even the slightest supply of trimer ($\approx$0.001) is sufficient to sustain the catalytic activity. The lower half of the figure shows the situation when the probability of monomer desorption is introduced into the first environment of model 2. The value of y_1 remains constant at $\approx$0.185. However, with increase in P_A, the values of y_2 increase towards higher monomer partial pressure until $P_A = 0.10$ and thereafter attain the situation observed in the ER model, i.e. y_2 takes a fixed value. For $P_A > 0.10$, a continuous production of AB starts the moment $y_A > 0.185$ and it continues until the supply of trimer is switched off. Therefore, like the ER model, there is a large region over which the system shows a maximum reactive window width. The fact that a lower value of P_A is required in model 2 to sustain catalytic activity points out that the reactivity of the monomer is higher in the precursor model than in the ER model. This is logical because in the ER model the monomer can only react on the selected empty site S whereas in model 2 the precursor can also react with any of the nn sites of S, so even a small amount of the trimer is sufficient to sustain the catalytic activity.

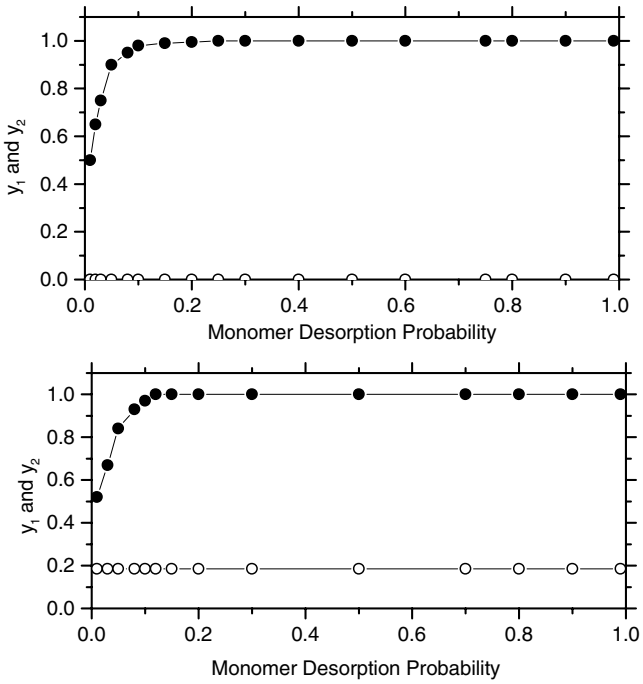

Figure 7. The values of transition points y_1 (open circle) and y_2 (solid circle) as a function of monomer desorption probability for model 1 (top) and model 2 (bottom).

4. Conclusions

We have studied ER and precursor models for a hypothetical MT reaction system on a square lattice. It has been seen that introduction of ER process in the LH model changes the situation significantly. The continuous phase transition of the LH model is eliminated, steady window width is widened and production rate is enhanced significantly. The productive activity starts the moment y_A departs from zero and a discontinuous transition point terminates the activity. The qualitative nature of the phase diagram remains same as observed in the MD ER model [19, 31]. It has also been seen that the introduction of a precursor mechanism along the lines envisaged by Harris and Kasemo [20] adds some interesting features to the phase diagram of the catalysed MT reaction system. When the motion of the precursor A^P is considered up to the first environment, the qualitative nature of the phase diagram is similar to that of the LH model. The introduction of precursor motion does not affect the continuous transition point. However, the discontinuous transition point is shifted to a value which is higher than the value observed in the LH model [6]. This situation has a close qualitative agreement with that observed by Khan *et al* [30]. The width of the reactive region increases if the mobility of the precursor is extended to the second and third neighbourhoods. The continuous transition disappears when precursor motion is extended up to the third-nearest neighbourhood. In addition, the value of the discontinuous transition in the third environment is very similar to that observed by Evans [29] for the ZGB model when he considered a large diffusion rate of the monomer. This situation is also in agreement with the MD model of Khan *et al* [30]. We conclude from our discussion that both our MT models resemble their respective MD models, which is the key feature of this study.

In both our models the dependence of the reaction rate on y_A can be fitted through simple mathematical relations (second-order polynomial and exponential growth). In a real experimental situation, the productive activity strongly depends upon temperature. In our simulations the temperature is involved through desorption of monomers from the surface. It has been observed that diffusion of the monomer does not change the qualitative nature of the situation of a particular model. However, the window width and production rate of AB increase in the two models. The value of y_2 shifts towards a higher value of y_A with increase in d_A. Desorption also plays the same role, with the difference that y_2 is eliminated in some cases.

In our opinion, lattice gas non-thermal LH models lead to a better and more realistic account of heterogeneous catalysed reactions. The present study has provided a good theoretical understanding for a hypothetical MT model. This theoretical study will be helpful to understand some real MT and DT models such as the gas phase shift reaction and the industrial preparation of methanol.

References

[1] Ziff R M, Gulari E and Barshad Y 1986 *Phys. Rev. Lett.* **56** 2553
[2] Dumout, Poriaux M and Dagonnier P 1986 *Surf. Sci.* **169** L307
[3] Meakin P and Scalapino D J 1987 *J. Chem. Phys.* **87** 731
[4] Khan K M, Yaldram K and Ahmed N 1998 *J. Chem. Phys.* **109** 5054
[5] Kohler J and ben-Avraham D 1991 *J. Phys. A: Math. Gen.* **24** L621
[6] Khan K M, Basit A and Yaldram K 2000 *J. Phys. A: Math. Gen.* **33** L215
[7] Khan K M, Basit A and Yaldram K 2000 *Surf. Sci.* **469** 65
[8] Albano E V 1992 *Phys. Rev. Lett.* **69** 656
[9] Albano E V 1992 *J. Phys. A: Math. Gen.* **25** 2557
[10] Khan K M, Yaldram K, Ahmad N and Qamar-ul-Haque 1999 *Physica* A **268** 89
[11] Yaldram K and Khan M A 1991 *J. Catal.* **131** 369
[12] Meng B, Weinberg W H and Evans J W 1993 *Phys. Rev.* E **48** 3577
[13] Khan M A, Yaldram K, Khalil G K and Khan K M 1994 *Phys. Rev.* E **50** 2156
[14] Yaldram K, Khan K M, Ahmad N and Khan M A 1994 *J. Catal.* **147** 96
[15] Khan K M and Yaldram K 2000 *Surf. Sci.* **445** 186
[16] Khan K M, Khalifeh J, Yaldram K and Khan M A 1997 *J. Chem. Phys.* **106** 8890
[17] Khan K M and Ahmad N 2001 *Chem. Phys. Lett.* **339** 179
[18] Jackson B and Persson M 1995 *J. Chem. Phys.* **103** 6257
[19] Meakin P 1990 *J. Chem. Phys.* **93** 2903
[20] Harris J and Kasemo B 1981 *Surf. Sci.* **105** L281
[21] Harris J, Kasemo B and Tornqvist E 1981 *Surf. Sci.* **105** L288
[22] Wolf N O, Burgess D R and Hoffman D K 1980 *Surf. Sci.* **100** 453
[23] Khan K M, Albano E V and Monetti R A 2001 *Surf. Sci.* **482** 78
[24] Khan K M, Ahmad N and Albano E V 2001 *Surf. Sci.* **494** 111
[25] Gates C 1992 *Catalytic Chemistry* (New York: Wiley) p 359
[26] Engel T and Ertl G 1979 *Adv. Catal.* **28** 1
[27] Ehsasi M, Matloch M, Frank O, Block J H, Christmann K, Rys F S and Hirschwald W 1989 *J. Chem. Phys.* **91** 4949
[28] Khan K M and Ahmad N 2000 *Physica* A **280** 391
[29] Evans J W 1993 *J. Chem. Phys.* **98** 2463
[30] Khan K M and Albano E V 2002 *Chem. Phys.* **276** 129–37
[31] Khan K M and Ahmad W 2002 *J. Phys. A: Math. Gen.* **35** L2713